Subject No: 3

INHOMOGENEOUS BROADENING OF PAC SPECTRA WITH V_{zz} AND η JOINT PROBABILITY DISTRIBUTION FUNCTIONS

W.E. Evenson[1], M. Adams[1], A. Bunker[1], J. Hodges[1], P. Matheson[1], T. Park[1], M. Stufflebeam[1], and M.O. Zacate[2]

[1] Dept. of Physics, Utah Valley University, Orem, UT 84058, USA
[2] Dept. of Physics and Geology, Northern Kentucky University, Highland Heights, KY 41099, USA
zacatem1@nku.edu

The perturbed angular correlation (PAC) spectrum, $G_2(t)$, is broadened by the presence of randomly distributed defects in crystals due to a distribution of electric field gradients (EFGs) experienced by probe nuclei. Heuristic approaches to fitting spectra that exhibit such inhomogeneous broadening (ihb) consider only the distribution of EFG magnitudes V_{zz}, but the physical effect actually depends on the joint probability distribution function (pdf) of V_{zz} and EFG asymmetry parameter η. The difficulty in determining the joint pdf leads us to more appropriate representations of the EFG coordinates, and to express the joint pdf as the product of two approximately independent pdfs describing each coordinate separately. We have pursued this case in detail using as an initial illustration of the method a simple point defect model with nuclear spin $I=5/2$ in several cubic lattices, where $G_2(t)$ is primarily induced by a defect trapped in the first neighbor shell of a probe and broadening is due to defects distributed at random outside the first neighbor shell. Effects such as lattice relaxation are ignored in this simple test of the method. The simplicity of our model is suitable for gaining insight into ihb with more than V_{zz} alone. We simulate ihb in this simple case by averaging the net EFGs of 20,000 random defect arrangements, resulting in a broadened average $G_2(t)$. The 20,000 random cases provide a distribution of EFG components which are first transformed to Czjzek coordinates [1, 2] and then further into the full Czjzek half plane by conformal mapping. The topology of this transformed space yields an approximately separable joint pdf for the EFG components. We then fit the nearly independent pdfs and reconstruct $G_2(t)$ as a function of defect concentration. We report results for distributions of defects on simple cubic (sc), face-centered cubic (fcc) and body-centered cubic (bcc) lattices. The method explored here for analyzing ihb is applicable to more realistic cases.

I. Introduction

At sites of cubic symmetry, the primary contribution to the EFG comes from the presence of defects. The PAC signal from probe nuclei in a cubic lattice is therefore most strongly determined by a defect in the nearest neighbor position. However, defects scattered throughout the lattice necessarily contribute to the EFG at the location of the probe nucleus. Each probe samples a different EFG owing to the distinct environment in which it is located relative to the background distribution of defects. In elementary cases with no lattice distortions or relaxations, the EFG at any probe location in the point charge approximation is obtained by summing over the defects. For N defects in a crystal structure, the EFG is defined as

$$V_{ij} = \frac{Zeq_{eff}}{4\pi\epsilon_o}\sum_{k=1}^{k=N}\frac{\left(3x_{ki}x_{kj}-\delta_{ij}{r_k}^2\right)}{r_k^5}, \quad (1)$$

where the indices i and j run from 1 to 3 over the Cartesian coordinates, x, y and z, and q_{eff} is the effective charge of the defect. The PAC spectrum, G_2(t), is damped by the background distribution of defects, and the peaks in its Fourier spectrum, $G_2(\omega)$, are broadened. This is referred to as inhomogeneous broadening (ihb)[1].

In general, for arbitrary concentrations c of randomly distributed defects, the EFG tensor could be characterized by a joint probability distribution function describing its EFG components. Since the EFG tensor is traceless, there are only two independent components, or principal coordinates: V_1, V_2. In a system with defect concentration c, these two components could be characterized by an appropriate joint probability distribution function $P(c, V_1, V_2)$. With these two components known, and their joint probability function determined, ihb could be modeled in a PAC spectrum by integration

$$G_2(c,t) = \iint G_2^{sfd}(V_1,V_2,t)P(c,V_1,V_2)dV_1dV_2, \quad (2)$$

where $G_2^{sfd}(V_1, V_2, t)$ represents a PAC state arising from a particular assortment of random defects that give rise to specific EFG values, V_1 and V_2, at a particular defect concentration, c. The superscript "*sfd*" is a reminder that the largest contributor to the spectrum comes from a *single, fixed defect* in a near neighbor location. Physically, such a situation can arise when there is an attractive interaction between the PAC probe and the defect, in which case the probability of the defect being located in a nearest neighbor position is enhanced over the probability c that the defect is located at other lattice sites. $G_2^{sfd}(V_1, V_2, t)$ is therefore an implicit function of c through V_1 and V_2.

Typical parameterizations characterizing PAC have used V_{zz} and the asymmetry parameter $\eta = (2V_{xx}+V_{zz})/V_{zz}$ as if these were the two independent components implied by the zero-trace of the EFG tensor. However, V_{zz} and η are strongly correlated and not independent. Thus, the nominally suggestive joint pdf, $P_{Vzz}(c,V_{zz})\, P_\eta(c,\eta) dV_{zz}\, d\eta$, even if it were known, would not be the appropriate weighting function with which to model ihb. The pair V_{xx} and V_{zz} are an equally plausible choice but are also not independent and thus unsuitable.

In brief, examination of distributions of deviates of V_{zz} and V_{xx} reveal a strong correlation between the two. The deviates are confined to small, disconnected triangular wedges in the (V_{xx}, V_{zz}) plane. The reason for this was first addressed by Czjzek[2] and explained further by Butz[3]. Czjzek identified the multiple connectedness of V_{zz}, and η in amorphous solids by examining the limits imposed on the topology of the EFG coordinates through the constraint $0 \leq \eta = (2V_{xx}+V_{zz})/V_{zz} \leq 1$. In crossing the line defined by $\eta = 1$, V_{xx} goes to zero and V_{zz} changes sign. That result splits the regions of the (V_{xx}, V_{zz}) plane in which the EFG deviates are distributed. Czjzek proposed a new set of coordinates that reconnected the separate parts of the plane into a single, simply-connected 60 degree wedge bounded by $\eta = 0$ lines. The Czjzek transformation, as modified by Butz, is $V_{xx} = -Y/2$, $V_{vv}=-(\sqrt{3}\, X-Y)/4$, and $V_{zz}=(\sqrt{3}\, X+Y)/4$. We find that for our lattice structures, the Czjzek transformation alone does not remove the correlation between V_{zz} and η. However, a conformal mapping of the Czjzek wedge to the full half plane by defining the transformation, $W = Z^3$ or $(W_1+iW_2) = (X+iY)^3$, produces two approximately uncorrelated, independent coordinates[4]. We identify these coordinates as W_1 and W_2. Each is an explicit function of V_{zz} and η. For simplicity we suppress the notation for that dependence:

$$(3) \qquad W_1 = \frac{8}{3\sqrt{3}}\eta(9-\eta^2)|V_{zz}|^3 \quad \text{and} \quad W_2 = 8(1-\eta^2)V_{zz}^3.$$

With this transformation, the statistical properties of W_1 and W_2 may be separately investigated, and their individual probability distribution functions (pdfs) characterized. In particular, the dependence of each pdf on defect concentration may be studied. With the statistical correlation between W_1 and W_2 being weak, we approximate the joint probability distribution function as the simple product of the two individual and essentially independent pdfs,

$$(4) \qquad P_{12}(c,W_1,W_2) \equiv P_1(c,W_1)\, P_1(c,W_1).$$

We may then model the effects of ihb through the integral

$$(5) \qquad G_2(t,c) = \int_{-\infty}^{\infty}\int_0^{\infty} G_2^{sfd}(W_1,W_2,t)P_1(c,W_1)P_2(c,W_2)dW_1dW_2.$$

The ihb dependence on V_{zz} and η is now implicit through the definitions of the new EFG coordinates W_1 and W_2.

We have investigated this methodology for characterizing ihb by calculating the statistical distributions of V_{zz} and η for various concentrations of defects in simple cubic (sc), body-centered cubic (bcc) and face-centered cubic (fcc) lattices and then applying Eq. 3. Using Eq. 4, we have determined the concentration dependence of the joint pdf, $P_{12}(c,W_1,W_2)$. Using Eq. 5 we have modeled the concentration dependence of ihb on the PAC spectrum in these lattices.

In spite of the inexact equality implied in defining Eq. 4 due to the weak correlation of W_1 and W_2, we find as a matter of practice that Eq. 5 satisfactorily models ihb in all the simple models that we have studied.

We note that this method could potentially be applied to the analysis of problems in any hyperfine area whose physics is determined by the EFG tensor. It is certainly not limited to the oversimplified models reported here that we have used to explore the method. Likewise, it is not limited to $I = 5/2$ or any other of the specific properties of our illustrative models.

II. Model Calculations:

By characterizing the joint pdf as a function of W_1, W_2, and c, we are able to reproduce ihb in PAC spectra. We consider the merit of our procedure to be in the quality of the model fits to simulated PAC spectra.

For the purposes of exploring the proposed method, we consider only a simple point defect model in cubic structures for nuclear spin $I=5/2$. Lattice relaxations are ignored. All defects too have the same fixed charge, and we assume each probe has one, and only one, defect fixed in a near neighbor position. We assume an attractive interaction of some type between the probe and the defect, such that one, and only one defect inhabits the first near neighbor shell. We assume other defects to be randomly distributed and restricted only by their concentration, c. We model sc, bcc, and fcc lattices and study defect concentrations ranging from c = 0.1 % to c = 15%. For a given concentration and lattice we begin by calculating the EFG tensor for a random distribution of defects, and then we repeat the calculation 20,000 times, each time with a different random distribution of defects. At each step the EFG tensor is diagonalized to obtain, V_{xx} V_{yy} and V_{zz} from which we also define η. Each simulation thus gives for each lattice and concentration value, a set of 20,000 V_{zz} and η values for 20,000 distinctly different arrangements of random defects around the probe and its single, fixed near neighbor defect. Using each set of V_{zz} and η values, an average ihb-affected $G_2(c,t)$ is also calculated, and serves as the simulated data against which our reconstructed spectrum will be compared.

We then apply our Czjzek-conformal map, Eq. 3, to the set of 20,000 EFG parameters to obtain sets of W_1 and W_2. From these, we construct $P_1(c,W_1)$ and $P_2(c,W_2)$ by examining the normalized histograms of each distribution and treating each as if it were independent, as per our Eq. 4. By inspection and trial and error we determined the most appropriate functional forms for $P_1(c,W_1)$ to be gamma distributions, while $P_2(c,W_2)$ are well modeled by Levy alpha-stable distributions[5]. Gamma distributions are characterized by two parameters, the mean, $\mu=k\theta$ and standard deviation, $\sigma = k^{1/2}\theta$. Levy alpha-stable distributions are nominally characterized by four parameters, α, β, γ and δ. The latter two, γ and δ, are scaling values related to the distribution width and peak location. The parameter α, characterizes the nature of the distribution's tail and β is a skewness parameter influencing the overall symmetry of the distribution envelope. As a matter of practice, fitting ihb in PAC spectra would be impractical if six adjustable parameters were required. Fortunately, it is possible to characterize the pdf parameters' dependences on defect concentration c so that only the single parameter c is needed to characterize the ihb. To illustrate, we determine functional forms for the values $\mu(c)$, $\sigma(c)$, $\alpha(c)$, $\beta(c)$, $\gamma(c)$ and $\delta(c)$ by fits to simple, monotonic functions. In subsequent modeling of PAC spectra we use these functional fits to model the concentration dependence.

We are exploring the physical basis for the functional forms of the pdfs and their concentration dependence. These questions are not yet clearly resolved. We note that experimental fits to PAC data often report EFG distributions with functional dependences falling between those characterized by Cauchy-Lorentz distributions on one extreme and Gaussian on the other [6, 7 and 8]. Alpha-stable distributions model both extremes where Lorentz distributions result from taking α=1, and β=0, and Gaussian distributions from α = 2. We find in all cases for our simulations that for $P_2(W_2)$, α =1 for c=0% and that α saturates to about $\approx$ 1.8 for higher concentrations.

With $P_1(c,W_1)$, and $P_2(c,W_2)$, established in this manner, we model ihb by numerically integrating Eq. 5.

III. Results

In this paper we limit our fits to the range of defect concentrations from c = 0.1% to 15 %. For defect concentrations in this range, $P_1(c,W_1)$ and $P_2(c,W_2)$ have smooth, well-defined distributions that for increasing defect concentration have decreasing central peak amplitudes and increasing peak widths. At lower concentrations,

both distributions must approach delta functions in W_1 and W_2. While we see this tendency in our data, it is also true that at lower concentrations, there are marked "bumps" in the distribution away from the central peak, typically containing a few percent of the total probability density. We have found these to be associated with specific chance arrangements in the lattice at low defect concentration, but we have made no attempt to model these bumps and have normalized all our pdf fits to remove them. Otherwise, $P_1(c,W_1)$ and $P_2(c,W_2)$ are easily fitted by gamma distributions and alpha-stable distributions respectively.

Fig. 1 shows the pdf model fitted data for fcc $P_1(c,W_1)$ and $P_2(c,W_2)$ as discrete points as a function of concentration. Each parameter for both $P_1(c,W_1)$ and $P_2(c,W_2)$ is monotonic with concentration. The solid lines in the figure show our function fits to the parameter data. In the absence of sufficient theoretical guidance, we have fitted each data set with as simple a function as produced reasonable results. It is clear from the figure that a more complicated function could fit the data better. However, these models give reasonably satisfactory reconstructions of the PAC spectrum. The particular functional forms for the pdf parameter fits are given in Table 1. Most are modeled by simple power laws that vary with exponents between 0.5 and 0.75. However, the parameters α and β for $P_2(c,W_2)$ show a substantially different behavior. We have chosen to model each with a hyperbolic tangent. Both are steeply increasing functions at low defect concentration, but quickly saturate near c=3%. A value of $\alpha = 1$, $\beta = 0$ for the alpha-stable distribution yields a Lorentzian, with a tall narrow peak, and very long and broad tail, while for the saturated values of α nearing 2, the distribution is much closer to Gaussian. It is reasonable to assume that the largest contributions to ihb after the one fixed defect in shell 1come from those defects in shells 2 and 3. We interpret the rapid increase and then saturation of the α and β parameters to reflect a quick saturation of the contributions from these shells.

Our calculated pdfs for fcc 1, 3 and 10 % defect concentrations are shown in Fig. 2 along with our model fits. Those for bcc and sc are very similar and aside from slightly different scaling, show no substantive differences. Inspection of Table 1 adequately reveals the similarities between the different lattices. For brevity we choose not to display them here. It is readily apparent from Fig. 1 that our simplistic single formula fits should not be expected to provide exceptionally good fits over the whole range of defect concentrations. This is borne out in both Fig. 2 and Fig. 3 where the Table 1-formula-derived parameters for c=1% do not provide particularly good fits, although those at c = 3 and 10% are quite good. However, we have also included for comparison a fit to the 1% pdfs constructed from the fitted data points, also shown in Fig 1. This set of parameters, as originally derived from our simulations, fits the calculated 1% case very well so a more sophisticated parameterization of the concentration dependence can be expected to achieve results of this quality.

Figs. 3 and 4 present a comparison of the simulated PAC spectra and the reconstructed spectra using the models from Table 1 and Eq. 5, for c = 1, 3 and 10 %. Fig. 3 displays the results for fcc, while Fig. 4 displays comparisons for sc and bcc. Increased ihb with c is evident by the increased damping in the displayed graphs. Fig. 3 is for fcc and only differs from Fig. 4 by including for comparison a reconstructed $G_2(1\%,t)$ from the original data of Fig. 1 rather than from the Table 1 formulas, just as was done for the pdfs shown in Figure 2. Showing this best fit-case illustrates that regardless of a particular formula fit to the distribution parameters, our primary aim of finding topologically suitable EFG coordinates to characterize ihb is sound. We can readily and closely fit a $G_2(c,t)$ spectrum of arbitrary defect concentration given $P_1(c,W_1)$, $P_2(c,W_2)$ and Eq. 5.

IV. Conclusions

We have identified a workable topology for characterizing the joint pdf of two approximately independent EFG coordinates through a combination of a Czjzek transformation followed by a conformal mapping as described by Eq. 3. We have shown that $P_{12}(W_1,W_2)$, characterizing the modified EFG components $W_1(V_{zz},\eta)$ and $W_2(V_{zz},\eta)$, can be modeled over a broad range of defect concentrations from c = 0.1% to c = 15%, in a variety of lattice structures with two approximately statistically independent probability distribution functions as per Eq 4. We find that for elementary cubic structures, $P_1(c,W_1)$ is well represented by a gamma distribution, and $P_2(c,W_2)$ is characterized by the Levy alpha-stable distribution. By these means the dependence of ihb on both V_{zz} and η is implicit through the Czjzek-conformal map. It is evident from Eq. 3 that for small or moderate values of η, the two EFG coordinates W_1 and W_2 reflect the physics of η and V_{zz}, respectively, and thus show the importance of using a full, topologically appropriate representation of the EFG tensor in modeling *ihb*.

Given an experimental PAC spectrum $G_2(t)$ and a sufficiently realistic model for the EFG at the probe nuclei, it is possible to use our parameterization of the joint PDF to reconstruct $G_2(t,c)$ using Eq. 5, thereby providing a determination of the defect concentration in that experiment. These methods are readily generalizable to defects of varying effective charge and other crystal structures as long as the primary component of the $G_2(t)$ signal comes from a well-defined defect or lattice EFG plus a distribution of static defects.

Moreover there is nothing restricting the nature of our method to PAC. Other hyperfine techniques which rely on the EFG tensor should be amenable to using the same Czjzek-conformal map to construct an approximately separable joint PDF of topologically appropriate coordinates.

VI. Acknowledgements:

This work supported in part by NSF grant DMR-06-06006 (Metals Program).

VII. References:

[1] A. M. Stoneham, "Shapes of Inhomogeneously Broadened Resonant Lines in Solids", *Reviews of Modern Physics*, **41**, 82-108, (1969)

[2] Czjzek, G., "Distribution of Nuclear Quadrupole splittings in Amorphous Materials and the Topology of the (Vzz, η)-parameter space", *Hyperfine Interactions* 14(1983) 189-194.

[3] Butz, T. et al., "A New Approach in Nuclear Quadrupole Interaction Data Analysis: Cross-Correlation", *Physica Scripta* 54(1996) 234-239.

[4] Evenson, W. E., et al., "Topologically appropriate coordinates for (Vzz, η) joint probability distributions", in preparation.

[5] Nolan, J. P., "Stable Distributions – Models for Heavy Tailed Data", 2012, *Birkhauser*, Boston , In progress, Chapter 1 online at academic2.american.edu/$\sim$jpnolan

[6] Collins, G.S. and Sinha, P., "Structural, thermal and deformation-induced point defects in PdIn.", *Hyperfine Interact.* 130, 151-179 (2000)

[7] Gary S. Collins, Steven L. Shropshire, and Jiawen Fan, "Perturbed *g-g* angular correlations: A spectroscopy for point defects in metals and alloys," *Hyperfine Interactions* **62**, 1-34 (1990).

[8] Gary S. Collins, Luke S. J. Peng, and Matthew O. Zacate, "Point defects in FeAl studied by perturbed angular correlation," *Defect and Diffusion Forum* **213-215**, 107-132 (2003).

VIII Tables and Figures:

Table 1: For $P_1(c,W_1)$ characterized by mean, μ and deviance, σ:

	$\mu(c)$	$\sigma(c)$
bcc	$9.98c^{0.723}$	$6.50\ c^{3/4}$
sc	$12.3c^{0.6}$	$8.24\ c^{0.575}$
fcc	$45.6(1-\exp(-c/4.87))$	$7.35\ c^{1/2}$

For $P_2(c,W_2)$ characterized by α, β, and γ (δ = 64 in all cases).

	α	β	γ	δ
bcc	$1+0.71\tanh(c/1.93)$	$\tanh(c/2.85)$	$7.91c^{1/2}$	**64**
sc	$1+0.88\tanh(c/3.55)$	$\tanh(c/3.77)$	$9.03c^{1/2}$	**64**
fcc	$1+0.78\tanh(c/1.18)$	$\tanh(c/2.05)$	$24.8(1-\exp(-c/4.69))$	**64**

Table 1. Single fit parameterizations for the pdfs, $P_1(c,W_1)$ and $P_2(c,W_2)$. With no particular theoretical guidance to determine a model fit, we chose those simplest forms that adequately reproduced ihb over a broad range of defect concentration values. In general, the fits for concentrations c>1% are excellent. In all cases, it was found that fixing δ=64 (corresponding to V_{zz}=2, η=0) produced the best alpha-stable distribution fits to $P_2(c,W_2)$.

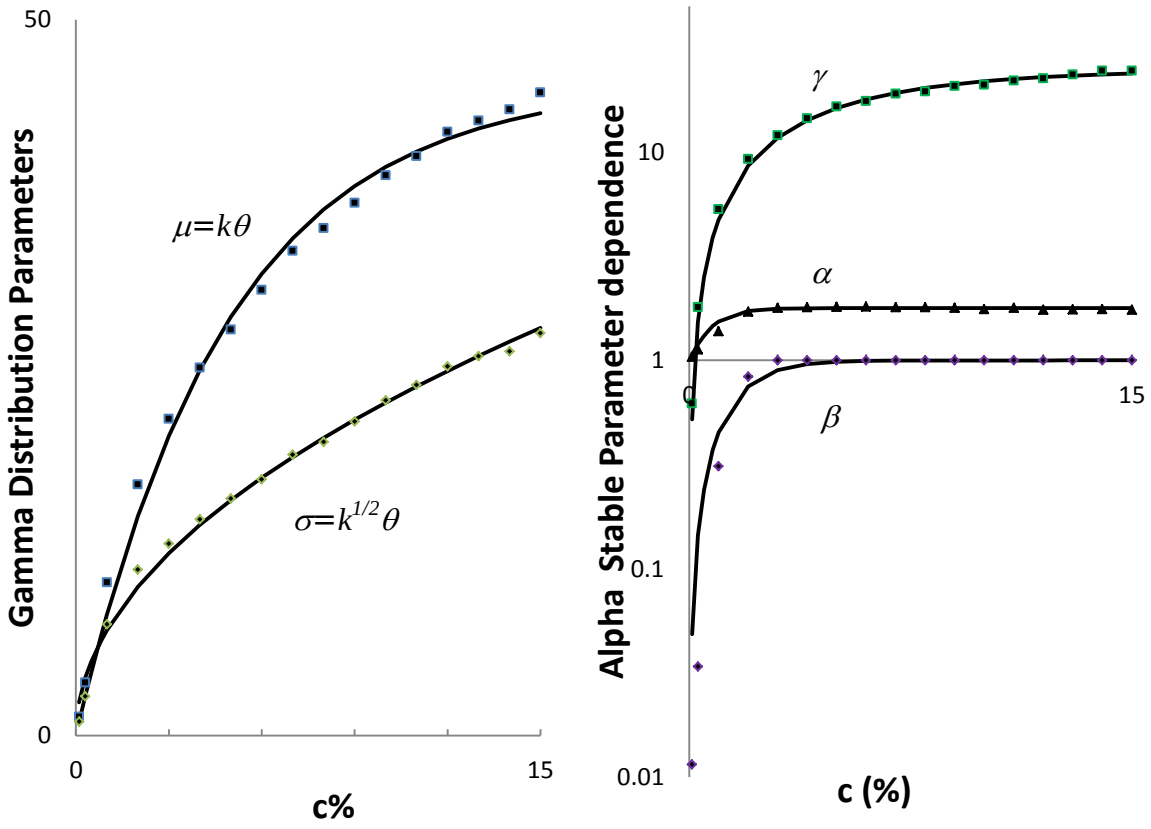

Figure 1. Concentration dependence of fit parameters for $P_1(c,W_1)$ and $P_2(c,W_2)$. Left: $P_1(c,W_1)$ is fitted with gamma distributions characterized by mean, μ and standard deviation σ. Right: $P_2(c,W_2)$ is fitted with Levy alpha-stable distributions with α, β and γ. The fourth parameter δ, is held fixed. The points mark the best individual fits of parameters to the simulated data. Solid lines show the single formula fits of Table 1. Parameter fits for sc and bcc are similar.

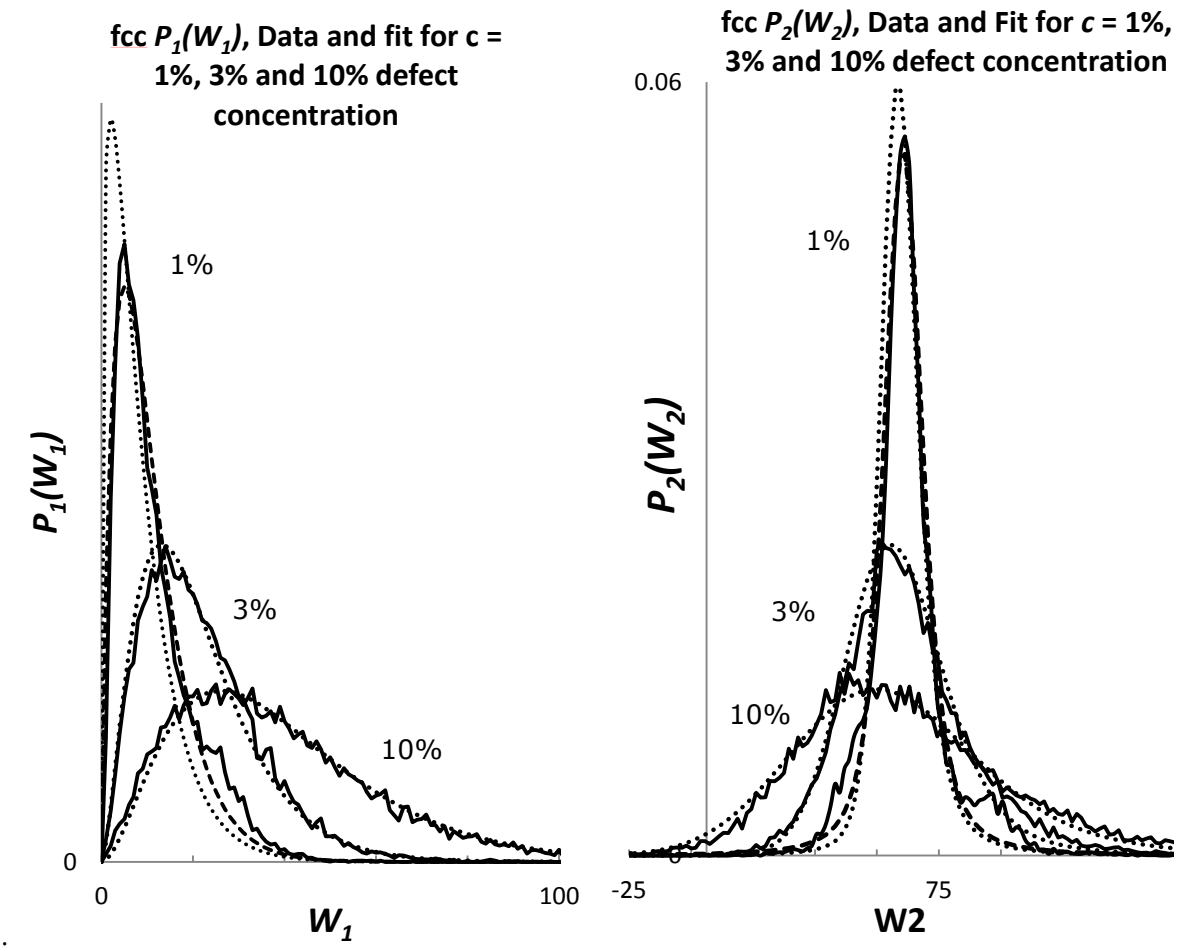

Figure 2: fcc pdfs and model fits for 1, 3 and 10% defect concentations. Left: $P_1(W_1)$, using gamma distributions. Right: $P_2(W_2)$ using Levy alpha-stable distributions. Solid lines are the pdfs constructed from the 20,000 deviates of our calculations. Model fits are shown by dotted lines. Inspection of Fig. 1 suggests that the concentation dependent parameter fits of Table 1are not optimal near c=1%. Shown for comparison by the dashed lines are the original fits for c= 1%. The pdfs for sc and bcc are similar.

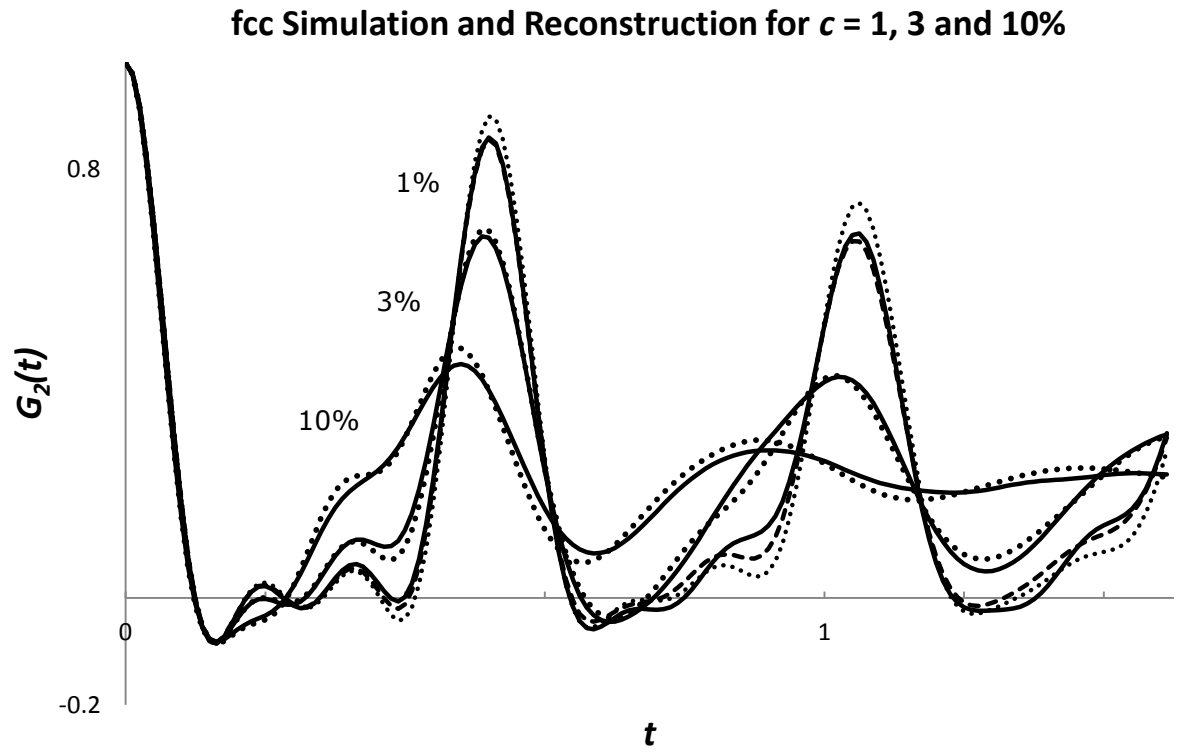

Figure 3. Comparison of fcc PAC spectra for 1%, 3% and 10 % defect concentrations. The curve associated with each concentration can be easily identified by observing that larger *c* results in greater damping, i.e, the 1% case is the most peaked, and the 10% case the least peaked, with the 3% case between the two. Data are derived from our original simulations and are shown by solid lines; models shown by dotted lines are reconstructed using Eq. 5 and the single formula fits of Table 1. The single dashed line for 1% shows a best fit case for comparison, showing that regardless of a particular general parameterization (Table 1), the method of characterizing a joint pdf for our transformed EFG coordinates W_1 and W_2 reproduces ihb with good accuracy.

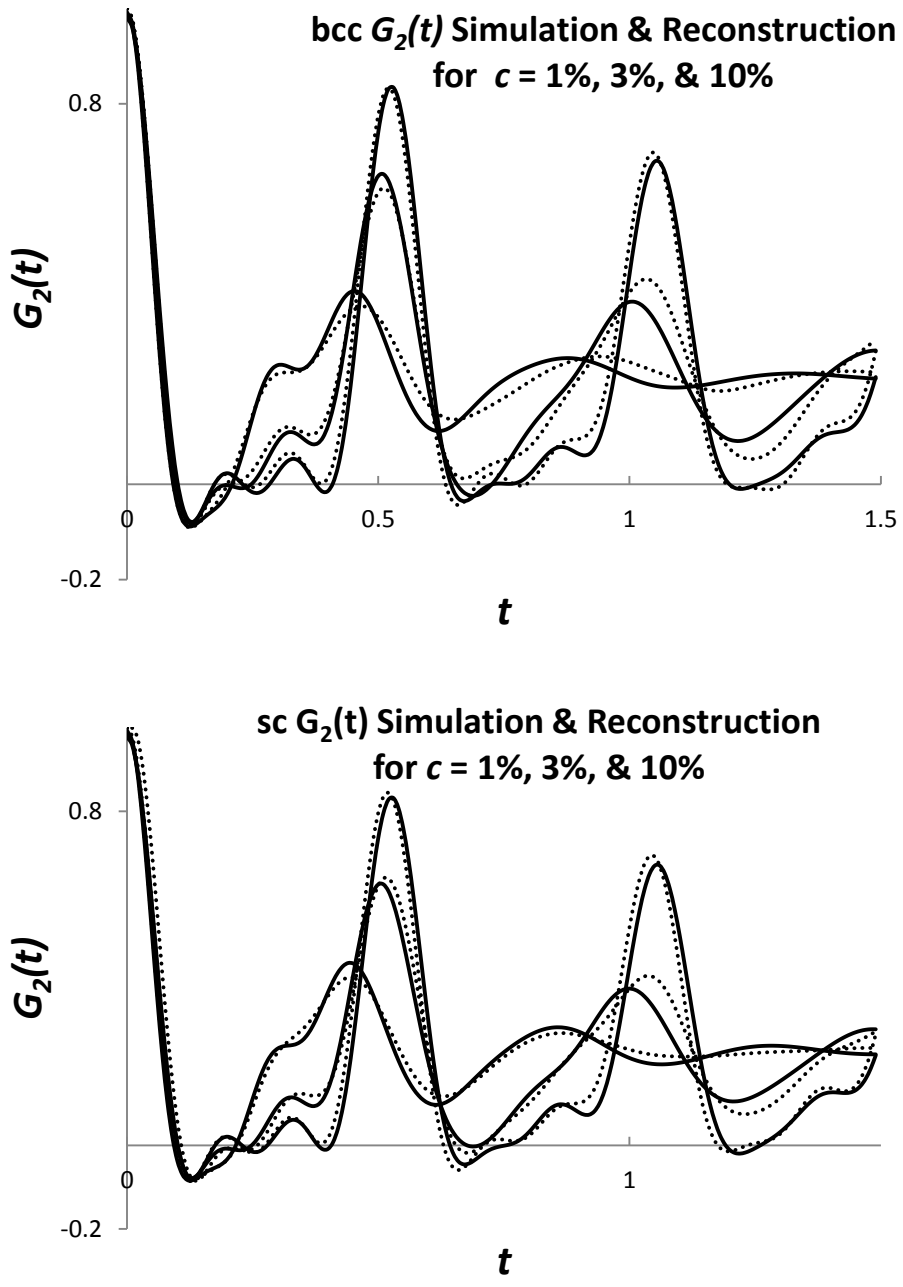

Figure 4. Comparable to Figure 3; Reconstructions for 1, 3 and 10% (dotted lines) and bcc (upper figure) and sc lattices (lower figure) using the single formula fits from Table 1 and Eq. 5. Fits are reasonably good, but moreover, the process of characterizing the joint pdf via Eq. 4 adequately models ihb in PAC spectra in a variety of cubic lattices.